Electrodynamic Trapping of Spinless Neutral Atoms with an Atom Chip

T. Kishimoto,[1,*] H. Hachisu,[2] J. Fujiki,[2] K. Nagato,[3] M. Yasuda,[2,†] and H. Katori[1,2,‡]

[1]*PRESTO, Japan Science and Technology Agency, Bunkyo-ku, Tokyo 113-8656, Japan*
[2]*Department of Applied Physics, School of Engineering, The University of Tokyo, Bunkyo-ku, Tokyo 113-8656, Japan*
[3]*Department of Engineering Synthesis, School of Engineering, The University of Tokyo, Bunkyo-ku, Tokyo 113-8656, Japan*
(Received 1 December 2005; published 31 March 2006)

Three-dimensional electrodynamic trapping of neutral atoms has been demonstrated. By applying time-varying inhomogeneous electric fields with micron-sized electrodes, nearly 10^2 strontium atoms in the $^1S_0$ state have been trapped with a lifetime of 80 ms. In order to design the electrodes, we numerically analyzed the electric field and simulated atomic trajectories in the trap, which showed reasonable agreement with the experiment.

PACS numbers: 32.80.Pj, 32.60.+i, 39.25.+k

Coherent manipulation of atoms or ions in the vicinity of solid surfaces has attracted increasing interest as a promising tool for quantum information processing (QIP) because of their potential scalability and controllability of atoms or ions that work as qubits [1–4]. So far, two approaches, i.e., magnetic manipulation of atoms with miniaturized wire traps [5,6] and miniature Paul traps [1] for ions, have been demonstrated. Recent experiments, however, have witnessed that the coherence time of these trapped atoms or ions was shortened by electromagnetic interactions caused by thermal magnetic fields [7–10] or fluctuating patch potentials [11] appeared on the surface if the distance between the particle and the surface became smaller than 100 μm. To avoid these harmful influences and to have a lifetime nearly of a second, paramagnetic atoms need to be more than tens of microns apart from metal surfaces at room temperature [7–10]. A reported heating rate of ions [11] indicated stronger coupling of trapped ions to surface potentials than that of neutral atoms.

It has been pointed out that the best candidates for long-lived trap are spinless neutral atoms, which weakly interact with stray fields via the Stark effect [12,13]. Alternatively, material dependence of the trap lifetime has been investigated to reduce thermal magnetic field in magnetic atom chips [9,10,14]. Electric manipulation of atoms, which allows manipulating spinless neutral atoms in addition to paramagnetic atoms and molecules, may open up a new possibility for scalable quantum systems with long coherence time. In this Letter, we demonstrate three-dimensional (3D) electrodynamic trapping of laser-cooled Sr atoms in the $^1S_0$ state with miniature electrodes fabricated on a glass plate. The very thin electrodes ($\sim$40 nm) used in the experiment will significantly reduce thermal magnetic fields near metal surfaces, which would be especially profitable in applying this scheme to paramagnetic atoms.

For an applied electric field $\mathbf{E}(\mathbf{r})$, the Stark energy is given by $U(\mathbf{r}) = -\frac{1}{2}\alpha|\mathbf{E}(\mathbf{r})|^2$. Since the static dipole polarizability α is positive for atoms in stable states, these atoms can be trapped at a local maximum of the electric field strength and behave as a "high-field seeker." However, as the Laplace equation does not allow an electrostatic field to form a maximum in free space, 3D trapping is not possible for a static electric field alone [15]. In addition, owing to a small dipole polarizability, rather high electric fields are required for the Stark manipulation of laser-cooled atoms: So far 1D or 2D focusing or trapping experiments [16–18] have been demonstrated by applying several to 10 kV to electrodes with dimensions of a few mm. A dynamic stabilization scheme, as employed in rf ion traps, allows electric trapping with higher dimensions. Electrodynamic 2D focusing of atoms [16] and guiding of molecules [19] were demonstrated by using 4 rods with oscillating voltages. 3D trapping by 3 phase electric-dipole fields [20] or by an oscillating hexapole field superimposed on a static homogeneous field [21] has been proposed. The latter scheme has recently been demonstrated in trapping cold polar molecules [22].

Here we consider 3D electrodynamic trapping with a two-phase electric-dipole field, which will allow planar geometry that is suitable for use with atom chips [23]. In order to illustrate the scheme, we first assume two spherical electrodes with radius b placed at $\pm d$ either on the x or y axis, kept at voltages $\pm V_0$ as shown in Fig. 1(a). The corresponding Stark energy u_x (or u_y) for an atom near the origin is calculated in the lowest order of $|x/d|, |y/d|, |z/d| \ll 1$,

$$\begin{pmatrix} u_x \\ u_y \end{pmatrix} \approx \frac{1}{2}m\omega_0^2 \begin{pmatrix} -\eta x^2 + y^2 + \xi z^2 - d^2/3 \\ x^2 - \eta y^2 + \xi z^2 - d^2/3 \end{pmatrix}, \quad (1)$$

where m is the atomic mass and $\omega_0 = (2bV_0/d^3)\sqrt{3\alpha/m}$ is the trapping frequency of an atom perpendicular to the dipole axis. The axial symmetry of electrodes determines $\eta = 2$ and $\xi = 1$. The static dipole polarizability of $\alpha = 3.08 \times 10^{-39}$ J/(V/m)^2 [24] for Sr atoms in the $^1S_0$ ground state is used in the calculation. While both of the potentials u_x and u_y provide static confinement along the z
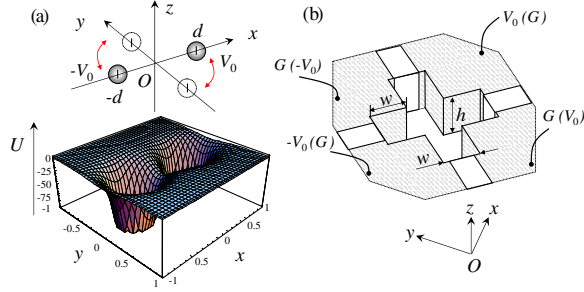
FIG. 1 (color online). Configuration of electrodes. (a) For analytic calculation, we assume two sphere electrodes applied with $\pm V_0$ and located at $\pm d$ on the x axis, which produce Stark potential of u_x as plotted below. (b) Actual electrodes are fabricated on a glass plate of thickness h, with through-hole crossed channels of width w. The shaded regions are silver coated to form electrodes, which are set to either $\pm V_0$ or ground level (G). Atoms will be trapped at the center of the through hole.

axis, they form saddle potential in the xy plane. The 3D trapping, therefore, can be realized by dynamically stabilizing atomic trajectories in xy plane by alternating these two potentials. In Eq. (1) anharmonic terms higher than $r_i^2 r_j^2/d^4$, where r_i and r_j stand for x, y, z coordinates, are neglected. However, as discussed later, these terms play a crucial role in determining the effective trap volume.

By switching the charge distribution between the x and the y axis at a period of $T/2$, the time-dependent Stark potential is given by

$$U(\mathbf{r}, t) = \begin{cases} u_x(\mathbf{r}); & nT \leq t < (n + \frac{1}{2})T, \\ u_y(\mathbf{r}); & (n + \frac{1}{2})T \leq t < (n + 1)T, \end{cases} \quad (2)$$

where n is an integer. The time evolution of the position and velocity of an atom subjected to $U(\mathbf{r}, t)$ can be described by transfer matrices [18,25], whose eigenvalues of $|\varepsilon| \leq 1$ guarantee stable trapping. The harmonic approximation of the Stark potential as given in Eq. (1) is used to determine the stability of the trap with respect to the driving frequency $f_0 \equiv 1/T$. For the electrodes configuration with $\eta = 2$ (and $\xi = 1$), as discussed above, the stability regime is calculated to be $1.56 < 2\pi f_0/\omega_0 < 1.80$ [23] [see Fig. 2(a)]. This narrow stability regime for f_0, however, made experiments rather challenging.

The stability regime on f_0 can be extended by reducing the normalized strength η of the antitrapping potential, as shown by a gray area in Fig. 2(a). Wider driving frequency range can be obtained for η close to unity, which is realized by applying line charges instead of point charges. Figure 1(b) depicts a model for designing actual electrodes, where the shaded parts are made of conducting material and the other parts are the insulator. When voltages are applied to four rectangular parallelepiped electrodes with diagonal separation of $\sqrt{2}w$ and thickness of h, most of the charges distribute at the ridge of the electrodes. Therefore the Stark potential can be approximated by line charges of length h.
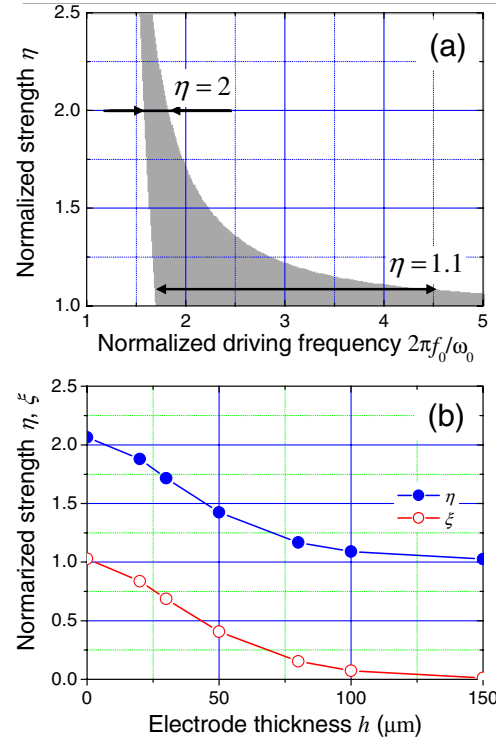

FIG. 2 (color online). (a) The shaded area shows the stable trapping regime with respect to the driving frequency f_0 and the relative strength η of antitrapping potential. The arrows indicate the stability region for $\eta = 2$ and $\eta = 1.1$. (b) Reduction of the normalized strength η (solid circles) of antitrapping and ξ (open circles) of static trapping as a function of the electrode thickness h for the channel width of $w = 50$ μm.

We numerically analyzed the electric field produced by these electrodes by employing the finite element method (FEM). Figure 2(b) shows the normalized strength of the antitrapping potential η (solid circles) and that of the static potential ξ (open circles) as a function of the electrode thickness h, where a channel width of $w = 50$ μm was assumed. For thinner electrodes, $\eta \approx 2$ and $\xi \approx 1$ were obtained in agreement with the case of two point charges [23] because the charge distributes at the tip of the electrode. By increasing the thickness of the electrodes, while the trapping frequency $\sqrt{\xi}\omega_0$ along z axis becomes weaker, η approaches unity and a wider stability region can be obtained, as expected for the two-dimensional atom guide [16,19].

Considering these trade-offs, we designed the thickness of the electrodes as $h = 100$ μm for $w = 50$ μm, which provided $\eta = 1.1$ [see Fig. 2(b)]. By applying voltages of $V_0 = 200$ V to the electrodes, $\omega_0 = 2\pi \times 2.9$ kHz and $\sqrt{\xi}\omega_0 = 2\pi \times 0.89$ kHz along the z axis were obtained. The latter is strong enough to support atoms against gravity even when the z axis directs vertically. The electrode assembly was made on a 100-μm-thick fused-silica substrate of 1 in. diameter, which was first coated with 250 nm thick silver on both sides. A cross through hole and electrode pattern were fabricated by the focused ion beam

process. Sidewalls of the hole were then coated with 40-nm-thick silver to form four electrodes. Figure 3(a) shows a scanning ion microscope (SIM) image of the atom chip.

An electrodynamic trapping experiment was performed in four steps, in less than 1 s: (1) laser cooling and trapping of ^{88}Sr atoms, (2) transport of atoms into an electric trap, (3) electrodynamic trapping, and (4) detection of trapped atoms. A schematic of an experimental setup is shown in Fig. 3(b). We cooled and trapped more than 10^4 atoms at several μK in 0.6 s by using a magneto-optical trap (MOT) on the $^1S_0$-$^3P_1$ spin-forbidden transition at $\lambda = 689$ nm [26]. Silver surfaces of the electrodes as shown in Fig. 3(a) were used as a mirror to perform a mirror MOT [6], in which the trapped atom cloud was located 1.5 mm below the mirror surface. This electrode assembly, or the "Stark chip," was glued on a 1-mm-thick, antireflection (AR) coated vacuum view port with a clear aperture of 8 mm. The vacuum pressure was typically 1×10^{-9} torr during the experiment.

The atoms were then loaded into a one-dimensional far-off-resonant optical lattice (FORL) formed by a pair of counterpropagating lasers at $\lambda_L \approx 810$ nm [27]. These lasers were focused onto the center of the through hole of the Stark chip. The $1/e^2$ waist radius was set to 16 μm so as to have the Rayleigh length of 1 mm to reach atoms in the MOT. Laser intensity of 100 mW per beam was chosen to provide a lattice potential with a radial confinement frequency of $\omega_r \approx 2\pi \times 1.2$ kHz at the chip center, which was close to a secular frequency of the electric trap as described below and allowed a good mode matching in atom loading into the electric trap. By changing the frequency of one of the lattice lasers [28], we adiabatically transported atoms into the atom chip in 6.8 ms. The transported atomic cloud inside the electrode gap had a temperature of about 7 μK and a $1/e^2$ radius of $r_{atom} \approx 7$ μm.

Turning off the lattice lasers, the electrodynamic trapping was started by applying $V_0 = 200$ V onto the diagonal electrodes [see Fig. 1(b)] at a driving frequency of $f_0 \approx 6.4$ kHz, which gave a secular frequency of ≈ 1.0 kHz. After a certain trapping time, the electric trap was switched
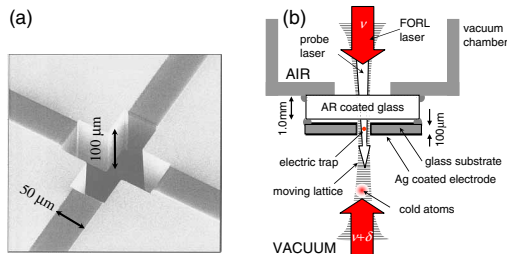
off. Using the moving lattice, we extracted the atoms 0.28 mm below the chip to observe trapped atoms. We illuminated them with a 10-μs-long probe laser resonant to the $^1S_0$-$^1P_1$ transition at $\lambda = 461$ nm. The fluorescence was imaged onto an intensified CCD camera to measure the number of trapped atoms with an uncertainty of 10%.

The solid circles in Fig. 4(a) show the number of trapped atoms as a function of the driving frequency f_0 for a trapping time of 5 ms. We have performed numerical integrations of the equation of motion of an atom subjected to the alternating electric fields [23] that were calculated by the FEM for the electrode configuration shown in Fig. 1(b). Taking the initial atom temperature and its spatial distribution as used in the experiment, the calculation (solid line) well reproduced the experiment, where the amplitude (atom number) was used as a fitting parameter.

As mentioned earlier the stability of the miniaturized electric trap is crucially affected by the anharmonicity of the trapping potential, since the Stark potential provided by the dipole electric field contains relatively large higher-order terms [29]. These terms limit the effective trap diameter $2r_{eff}$ to be typically one-fifth of the electrode separation $\sqrt{2}w$ as determined by numerical simulation

FIG. 3 (color online). (a) A SIM image of a Stark chip fabricated on a 100-μm-thick glass substrate. The dark and bright faces correspond to exposed glass and silver electrodes, respectively. (b) A schematic of the experimental setup. Laser-cooled ^{88}Sr atoms were transferred into an electric trap by a moving lattice. The electric trapping was performed while the moving lattice lasers were off.
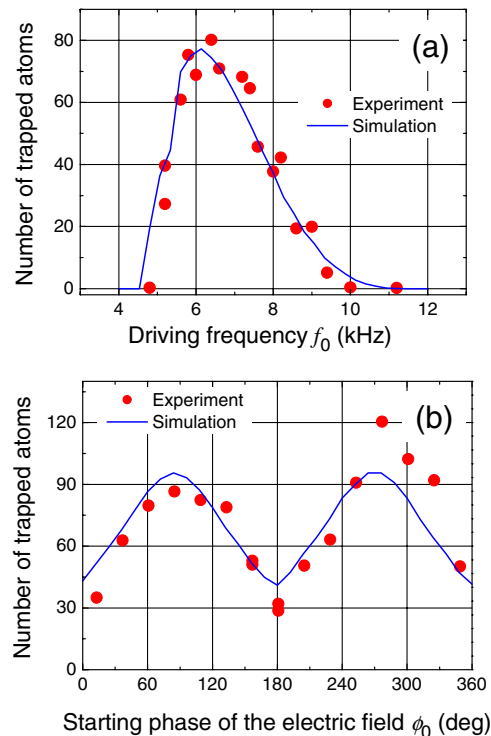

FIG. 4 (color online). The stability condition for the electrodynamic trapping. Atoms were trapped for 5 ms with driving voltages of $V_0 = 200$ V. Solid circles and solid lines show the experiment and simulation, respectively. (a) Number of trapped atoms as a function of the driving frequency f_0. The simulation took anharmonicity of the Stark potential into account. (b) Number of trapped atoms versus the starting phase ϕ_0 of the driving electric fields. An initial atomic cloud of 7 μK and $r_{atom} \approx 7$ μm were assumed in the simulation.

[23]. This limited trapping volume, in turn, makes the capture velocity v_c of the trap be dependent on a starting phase ϕ_0 of electric trapping field. Atoms with an outward velocity v_c toward a particular direction, say, the x axis, need to be decelerated by the driving field before reaching r_{eff} by the end of the trapping phase, while the similar but 180° out-of-phase discussion applies for the atomic motion in the y axis that is in the antitrapping phase. We defined $\phi_0 = 0$ when the Stark potential $U(\mathbf{r}, t)$ was switched at $t = nT$ as given in Eq. (2), i.e., $\phi_0 = \frac{t-nT}{T} \times 360°$ for the nth driving period, and studied the starting phase ϕ_0 dependent trap efficiency as shown in Fig. 4(b). The number of trapped atoms (solid circles) was in reasonable agreement with numerical simulation (solid line), where the amplitude (atom number) was used as an adjustable parameter, indicating that the best loading is realized for the trapping field started at $\phi_0 = 90°$ or $270°$. In the experiment, a slight asymmetry in the peak heights was observed. This may be attributed to spatial offset of an initial atomic cloud with respect to the trap center, which was possibly caused by misalignment of the FORL lasers. We have measured the lifetime of atoms in the electric trap to be 80 ms, which was in reasonable agreement with glancing-collisions-limited lifetime [30] assuming the background gas pressure of $\sim 10^{-8}$ torr in the electrode gap. Note that a similar lifetime was observed for atoms in the FORL, when its trap depth was comparable to that of the electric trap ($\approx 30\ \mu K$).

In applying atom traps to QIP experiments, qubit states should experience the same trapping potential so as to minimize decoherence caused by atomic motion [31,32]. For example, in the case of this Stark trap, $\pm m$ Zeeman substates of the $^3P_2$ metastable state, which has a lifetime over 100 s [33], can be used as a qubit state that experiences the same Stark shift. Although the coherent evolution of these states may be disturbed by the thermal magnetic fields that appeared on the electrodes surfaces, a very thin electrode (40 nm) demonstrated here may significantly reduce the thermal magnetic fields that cause spin flips [12,13], since the Johnson noise induced currents decrease as electrode's thickness [10]. Furthermore, since the operation of the electrodynamic trap relies on the switching of electric fields, it is free from Ohmic dissipation and allows dense integration of traps. Arrays of electrodes, four of which activated in turn so as to adiabatically transfer atoms, may constitute an atom waveguide that is reminiscent of the quantum CCD [34].

In conclusion, we have investigated the design of electrodes with a help of numerical simulation and demonstrated an electrodynamic trapping of spinless neutral Sr atoms with micron-sized structures. By reducing the electrode size to a few μm, these atom traps can be driven by a few volts [23], which will make electric atom traps compatible with electronic logic circuits, offering an interface between atom manipulation and electronics.

*Present address: Institute of Engineering Innovation, The University of Tokyo, Bunkyoku, Tokyo 113-8656, Japan.
†Present address: National Metrology Institute of Japan (NMIJ/AIST), Tsukuba, Ibaraki 305-8563, Japan.
‡Electronic address: katori@amo.t.u-tokyo.ac.jp

[1] D. Leibfried, R. Blatt, C. Monroe, and D. Wineland, Rev. Mod. Phys. **75**, 281 (2003).
[2] J. I. Cirac and P. Zoller, Phys. Rev. Lett. **74**, 4091 (1995).
[3] F. Schmidt-Kaler *et al.*, Nature (London) **422**, 408 (2003).
[4] D. Leibfried *et al.*, Nature (London) **422**, 412 (2003).
[5] J. Fortagh, A. Grossman, C. Zimmermann, and T. W. Hänsch, Phys. Rev. Lett. **81**, 5310 (1998).
[6] J. Reichel, W. Hänsel, and T. W. Hänsch, Phys. Rev. Lett. **83**, 3398 (1999).
[7] M. P. A. Jones, C. J. Vale, D. Sahagun, B. V. Hall, and E. A. Hinds, Phys. Rev. Lett. **91**, 080401 (2003).
[8] A. E. Leanhardt *et al.*, Phys. Rev. Lett. **90**, 100404 (2003).
[9] D. M. Harber, J. M. McGuirk, J. M. Obrecht, and E. A. Cornell, J. Low Temp. Phys. **133**, 229 (2003).
[10] Y. J. Lin, I. Teper, C. Chin, and V. Vuletić, Phys. Rev. Lett. **92**, 050404 (2004).
[11] Q. A. Turchette *et al.*, Phys. Rev. A **61**, 063418 (2000).
[12] C. Henkel and M. Wilkens, Europhys. Lett. **47**, 414 (1999).
[13] C. Henkel, S. Pötting, and M. Wilkens, Appl. Phys. B **69**, 379 (1999).
[14] C. D. J. Sinclair *et al.*, Phys. Rev. A **72**, 031603(R) (2005).
[15] W. H. Wing, Prog. Quantum Electron. **8**, 181 (1984).
[16] F. Shimizu, in *Atomic Physics 13*, edited by H. Walther, T. W. Hänsch, and B. Neizert (AIP, New York, 1993).
[17] P. Lemonde *et al.*, Europhys. Lett. **32**, 555 (1995).
[18] H.-R. Noh, K. Shimizu, and F. Shimizu, Phys. Rev. A **61**, 041601(R) (2000).
[19] T. Junglen, T. Rieger, S. A. Rangwala, P. W. H. Pinkse, and G. Rempe, Phys. Rev. Lett. **92**, 223001 (2004).
[20] F. Shimizu and M. Morinaga, Jpn. J. Appl. Phys. **31**, L1721 (1992).
[21] E. Peik, Eur. Phys. J. D **6**, 179 (1999).
[22] J. vanVeldhoven, H. L. Bethlem, and G. Meijer, Phys. Rev. Lett. **94**, 083001 (2005).
[23] H. Katori and T. Akatsuka, Jpn. J. Appl. Phys. **43**, 358 (2004).
[24] H. L. Schwartz, Phys. Rev. A **10**, 1924 (1974).
[25] M. W. Forbes *et al.*, J. Mass Spectrom. **34**, 1219 (1999).
[26] H. Katori, T. Ido, Y. Isoya, and M. Kuwata-Gonokami, Phys. Rev. Lett. **82**, 1116 (1999).
[27] H. Katori, T. Ido, and M. Gonokami, J. Phys. Soc. Jpn. **68**, 2479 (1999).
[28] M. BenDahan, E. Peik, J. Reichel, Y. Castin, and C. Salomon, Phys. Rev. Lett. **76**, 4508 (1996).
[29] The FEM analysis indicated that the contribution of the higher-order terms is on the order of 10^{-2} of the total potential energy for an atom at $r_{eff} = 8\ \mu m$ from the center.
[30] J. E. Bjorkholm, Phys. Rev. A **38**, 1599 (1988).
[31] H. Katori, M. Takamoto, V. G. Pal'chikov, and V. D. Ovsiannikov, Phys. Rev. Lett. **91**, 173005 (2003).
[32] P. Hyafil *et al.*, Phys. Rev. Lett. **93**, 103001 (2004).
[33] M. Yasuda and H. Katori, Phys. Rev. Lett. **92**, 153004 (2004).
[34] D. Kielpinski, C. Monroe, and D. J. Wineland, Nature (London) **417**, 709 (2002).